Phosphate and the Stabilization of Receptor-Receptor and Receptor-Ligand Interactions.

Shelley N. Jackson
National Institute on Drug Abuse
Intramural Research Program
National Institutes of Health

Protein-protein or peptide-peptide interactions are usually studied in the context of the lock and key model. We have found that linear interactions can play an important role in the formation of non-covalent complexes (NCX) in protein-protein as well as peptide-peptide interactions.

The following residues and modified residues are involved:

- **Arginine (Arg, R)**
- **Glutamate (Glu, E)**
- **Aspartate (Asp, D)**
- **Phosphorylated residues**
  - **Serine (Ser, S)**
  - **Threonine (Thr, T)**
  - **Tyrosine (Tyr, Y)**

The role of amino acid side chains and PTM in Protein-Protein and Peptide-Protein Interactions

Coulombic or Salt-Bridge formation: requires two or more adjacent **Arg** on one protein or peptide and two adjacent **Glu** or **Asp**, or a Phosphorylated (**p**) residue on the other

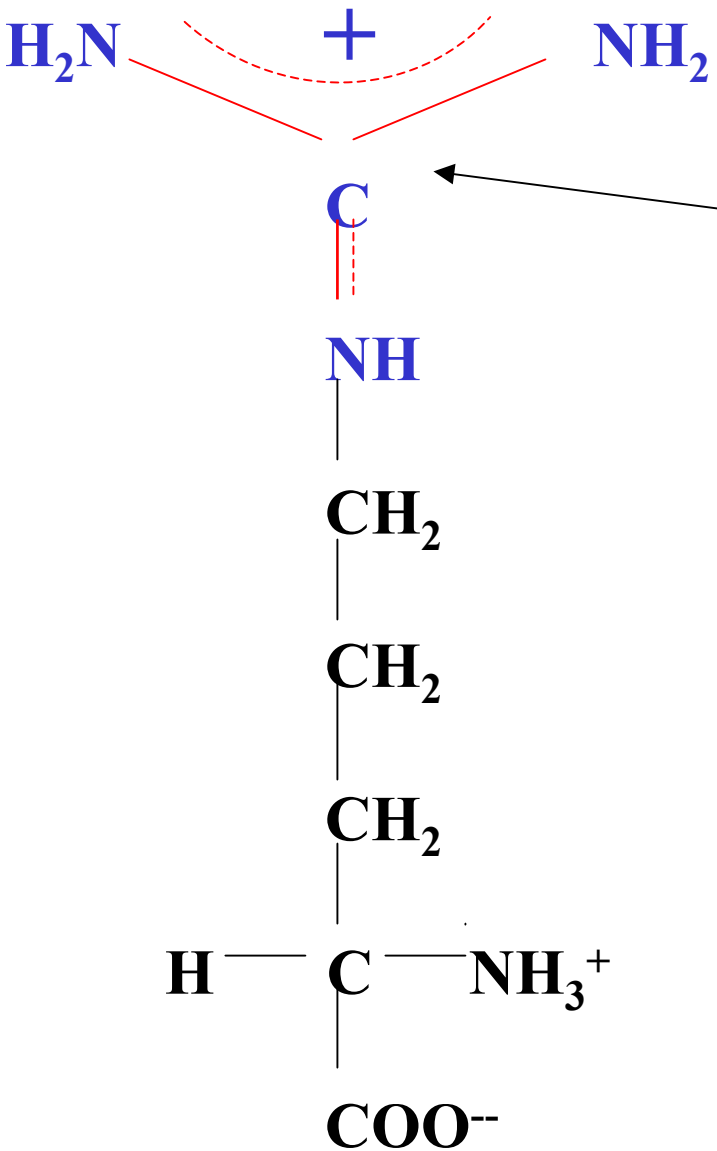

The Arginine side chain consists of three non-polar methylene groups and a **strongly basic δ-guanido group**:

- It has a **pKa of 12**.
- It is **ionized over the entire pH range** in which proteins exist naturally.
- It is **planar as a result of resonance** and the positive charge is effectively distributed over the entire group i.e. it is delocalized.

The side chains of Glutamic and Aspartic Acid differ only in having one and two methylene group respectively. The slight difference in length causes them to have different interaction with the peptide back bone. Hence Glu and Asp have different effects on conformation and chemical reactivity of the backbone.

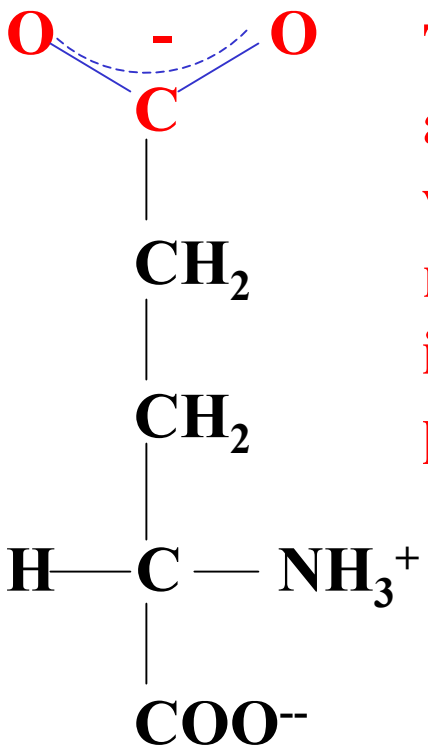

The carboxyl group of Glu and Asp ionize with pKa values of 4.3 and 3.9 respectively. They are ionized and very polar under physiological conditions.

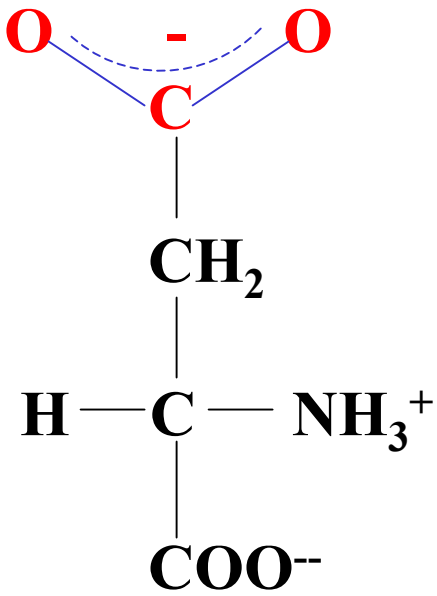

The Biological Magnets

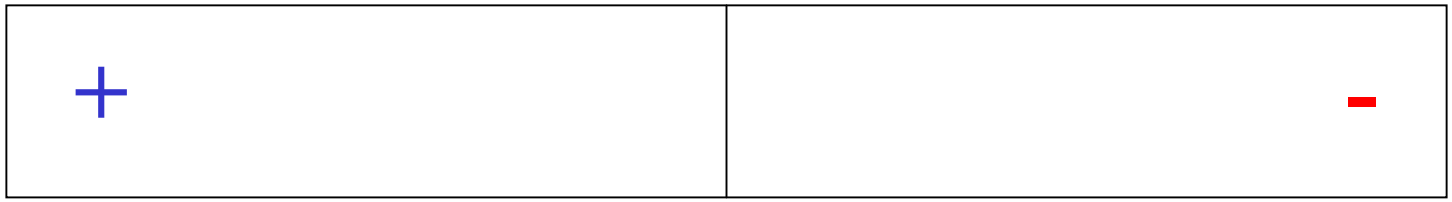

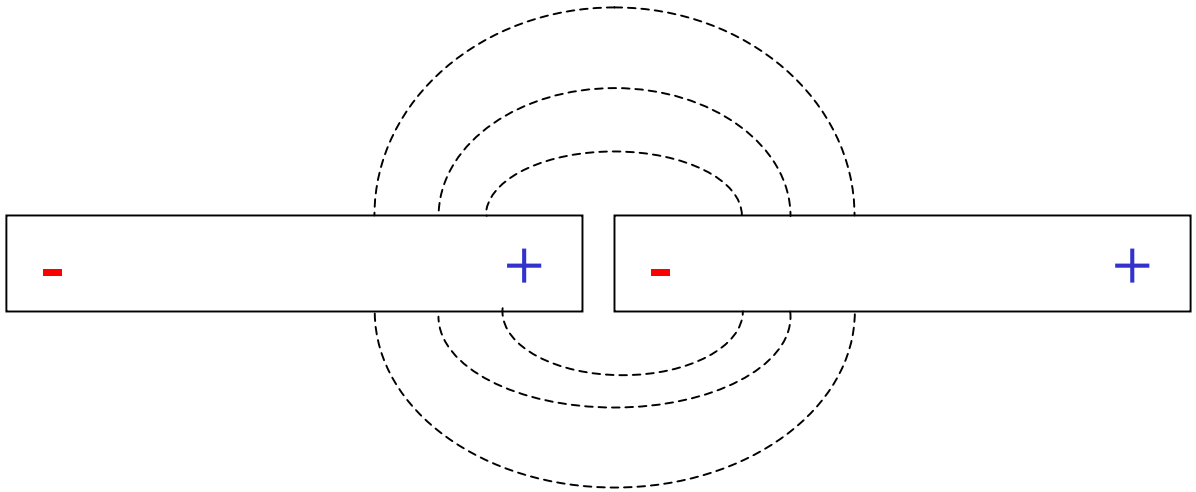

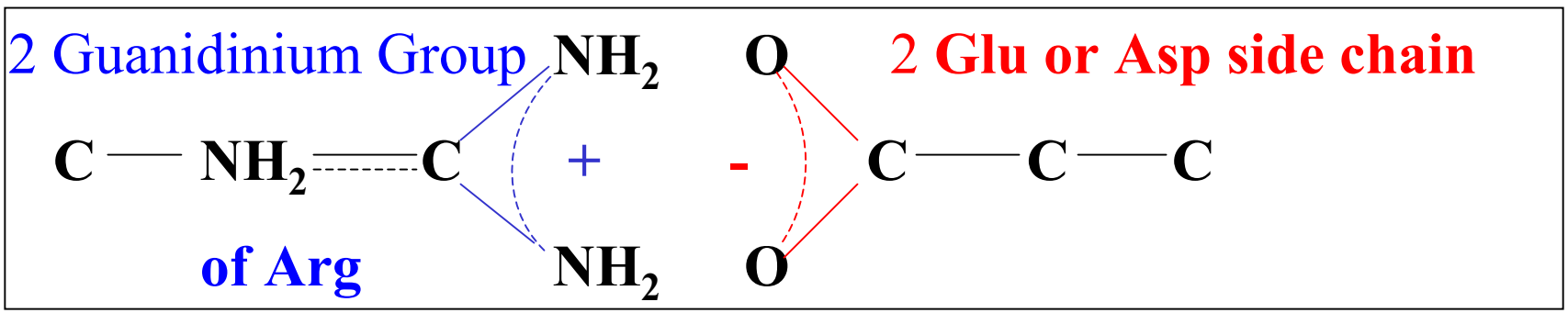

Phosphorylation

- One of the most common and important posttranslational modifications
- Functions as a molecular switch for signal transduction and enzyme catalysis
- Can occur on serine, threonine or tyrosine residues

Phosphorylated Amino Acid Residues

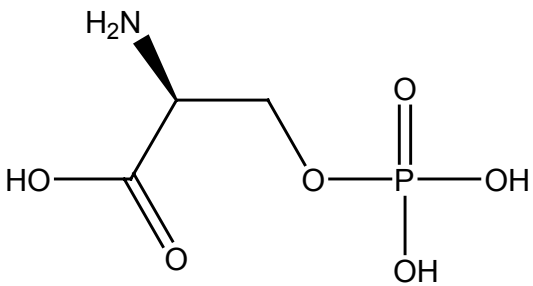

phosphoserine

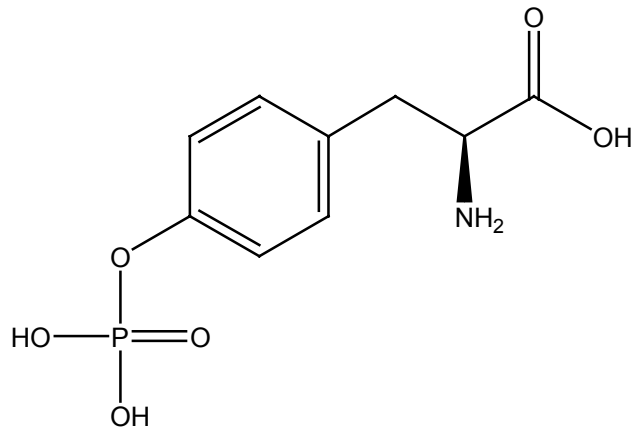

phosphotyrosine

The Biological Magnets

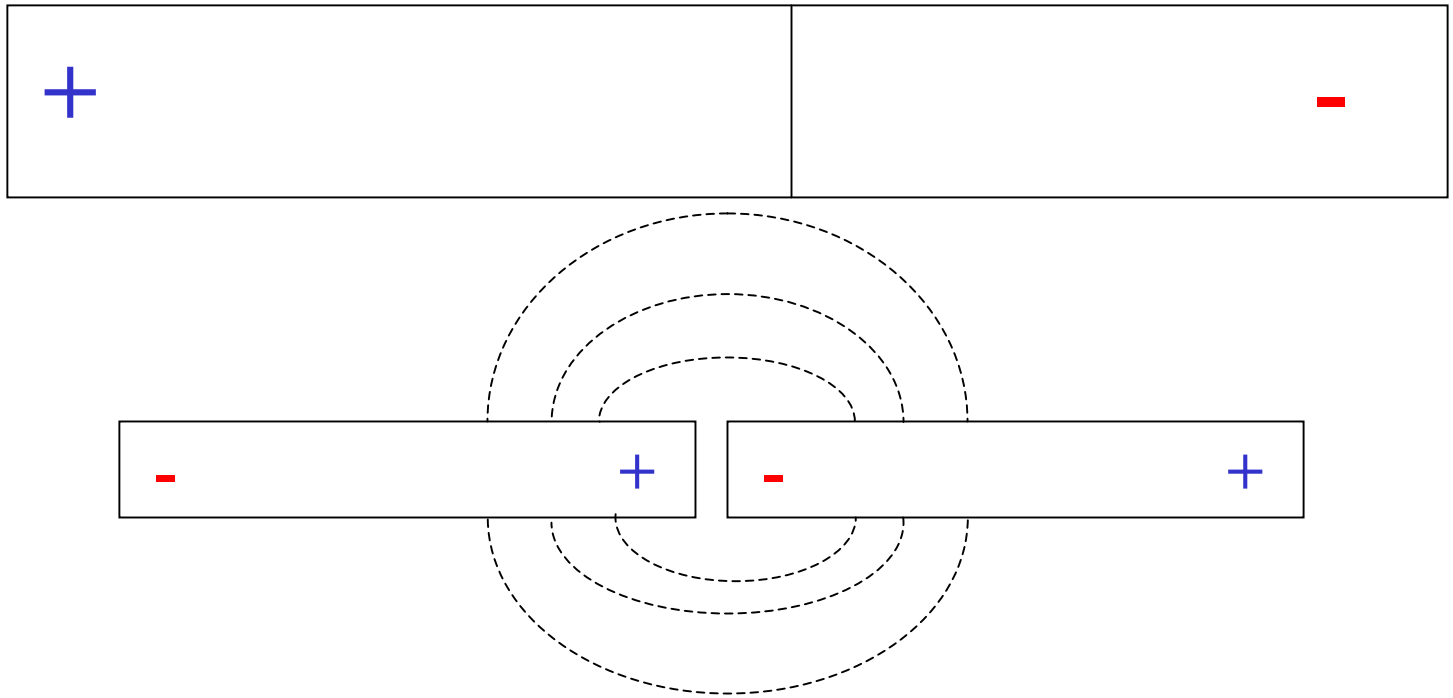

2 Guanidinium Group

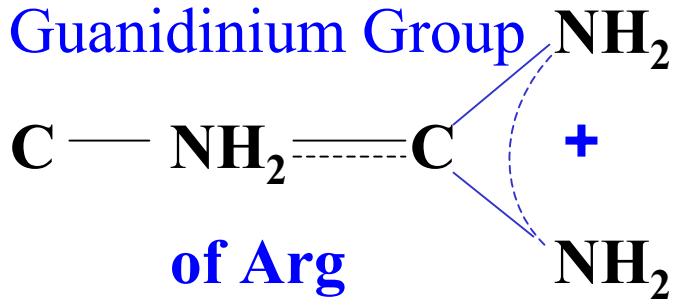

of Arg

1 Phosphate group

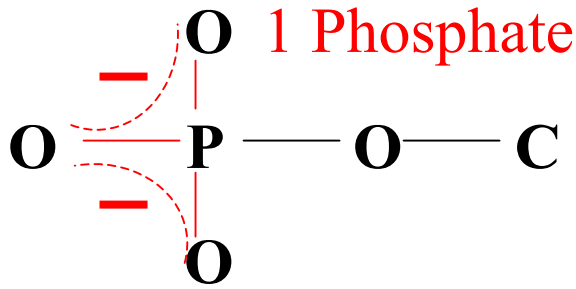

Comparative Study of the Stability of Glutamates and Phopshate in Intermolecular Interactions

- Receptor heteromerization results from the interactions of epitopes on two receptors.

- Basic epitope of the Dopamine D_2 third intracellular loop
  - **VLRRRRKRVN**

- Acidic epitope of the NMDA NR_1 subunit
  - KVNSEEEEEDA
  - KVNpSEEEEEDA
  - KVNpSAAAAAAA

MS/MS Experimental Setup.

Sample Mixtures	Selection Mass Window	Complexes Fragmanented
VLRRRRKRVN+KVNpSEEEEEDA	905 Da	$[NCX]^{3+}$ = 904.13 Da $[Dimer\ KVNpSEEEEEDA]^{3+}$ = 906 Da
VLRRRRKRVN+KVNSEEEEEDA	878 Da	$[NCX]^{3+}$ = 877.47 Da
VLRRRRKRVN+KVNpSAAAAAAA	793 Da	$[NCX]^{3+}$ = 792.79 Da

Note: 1. NCX = noncovalent complex formed between acidic and basic peptides.
2. Masses are monoisotopic.

Instrumental Parameters

- Q-TOF Global Ultima mass spectrometer in positive ion mode
- Flow rate of 5 μL/min
- Collision gas: Argon at 7psi
- Selection mass window of 6 Da

ESI-MS/MS of peptide mixture of 1 pmol/μL of VLR_4KRVN and 15 pmol/ μL $KVNpSE_5DA$

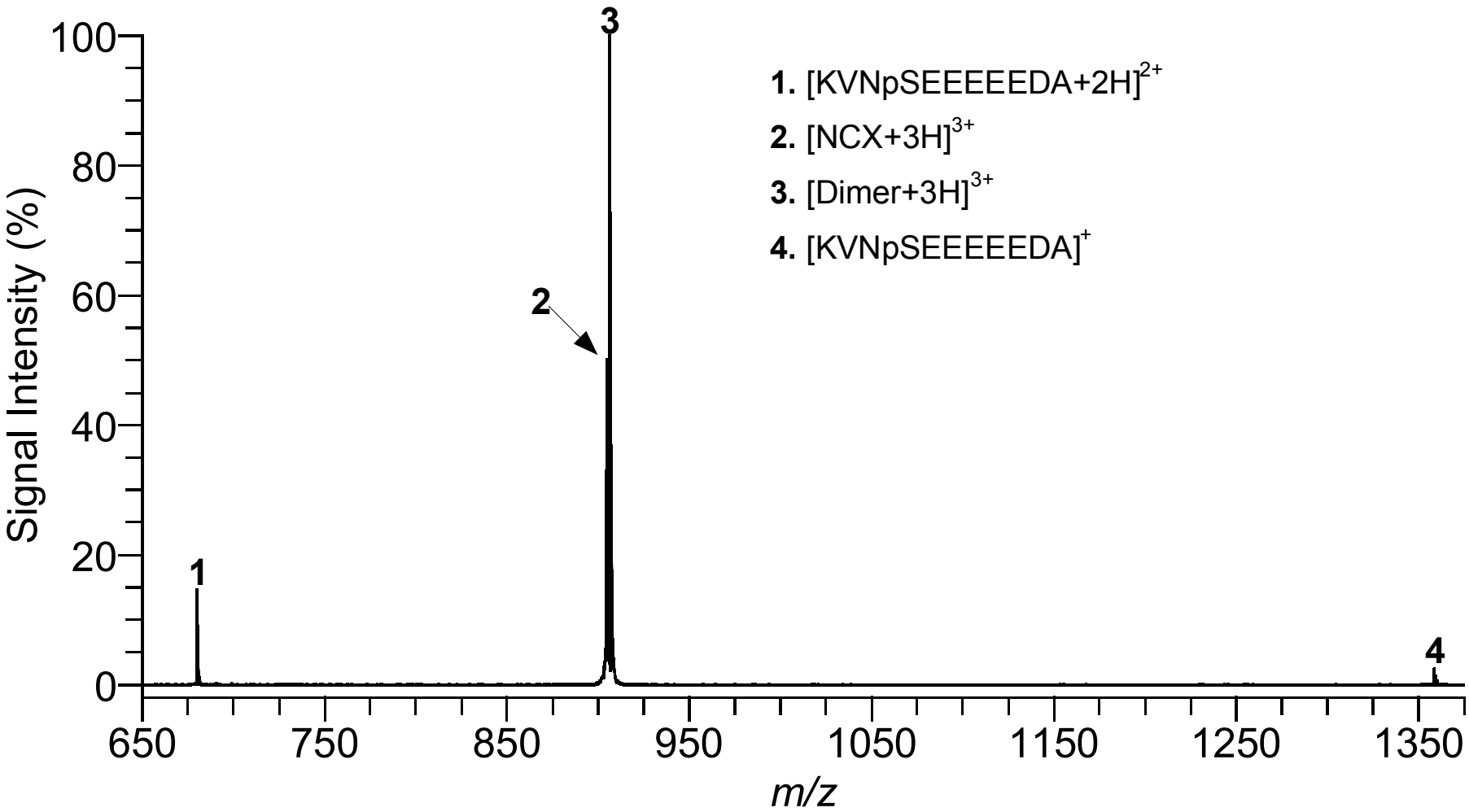

Mass Window = 905 Da Collision Energy = 5 V

ESI-MS/MS of peptide mixture of 1 pmol/μL of VLR_4KRVN and 15 pmol/ μL $KVNpSE_5DA$

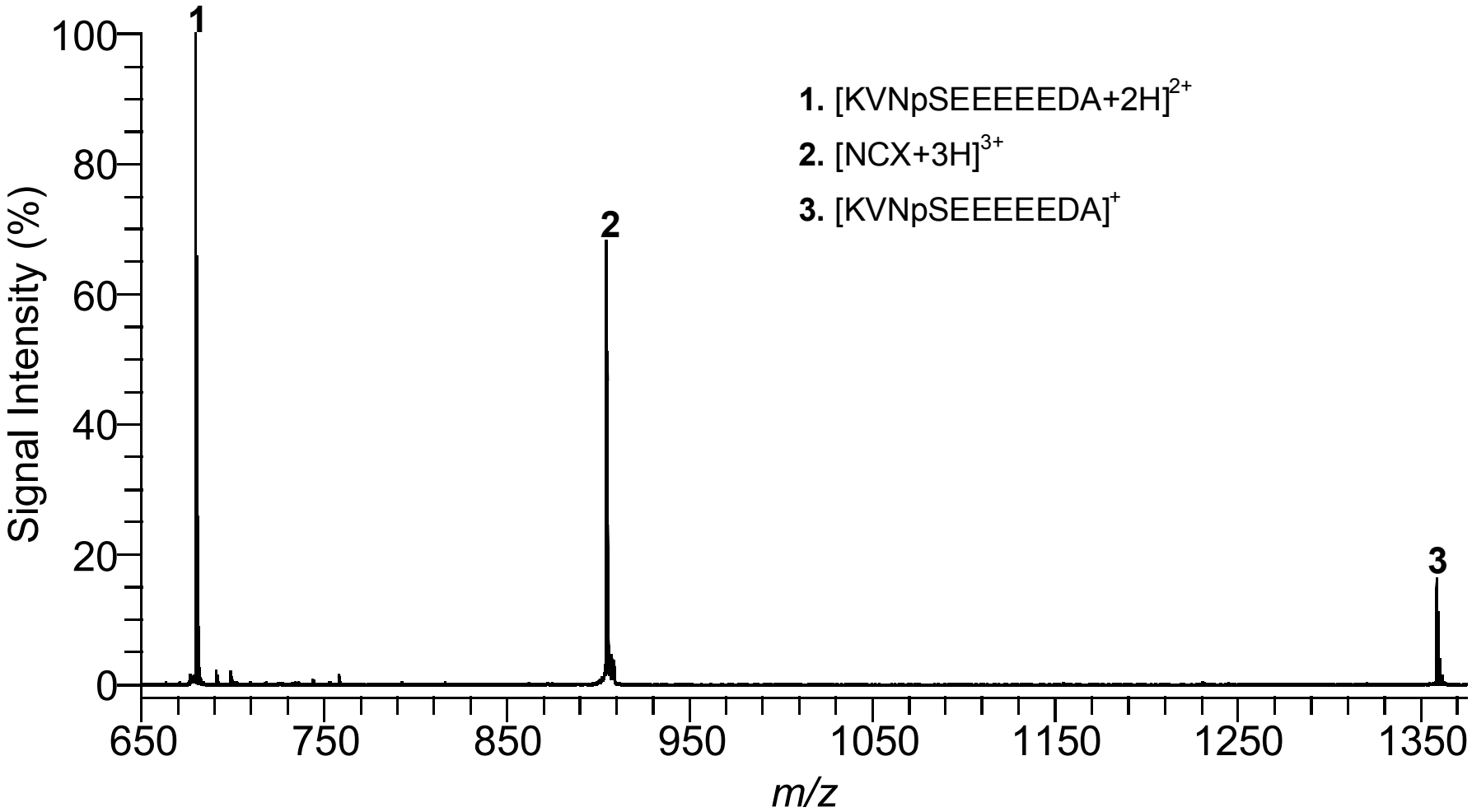

Mass Window = 905 Da Collision Energy = 15 V

ESI-MS/MS of peptide mixture of 1 pmol/μL of VLR_4KRVN and 15 pmol/ μL $KVNpSE_5DA$

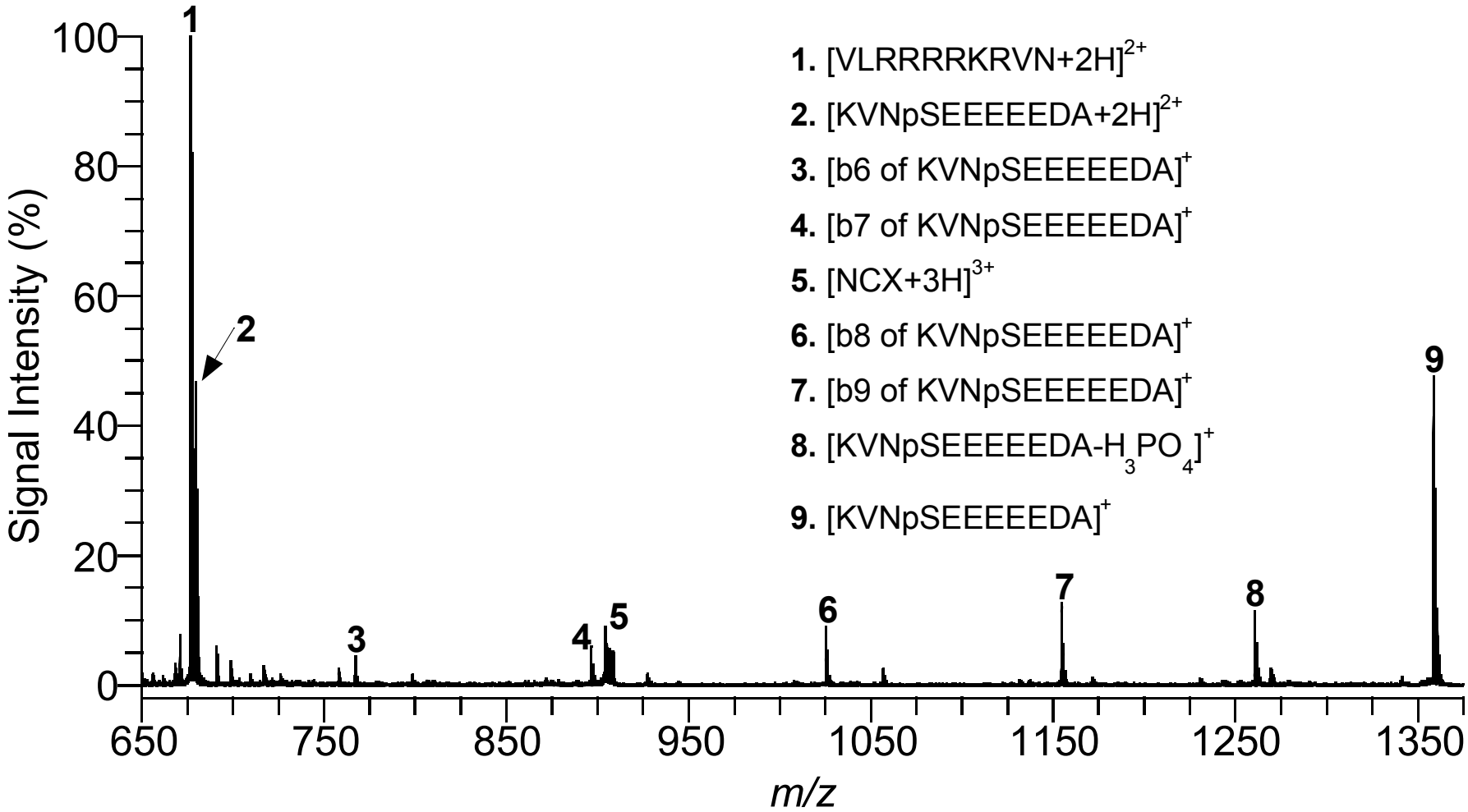

Mass Window = 905 Da Collision Energy = 30 V

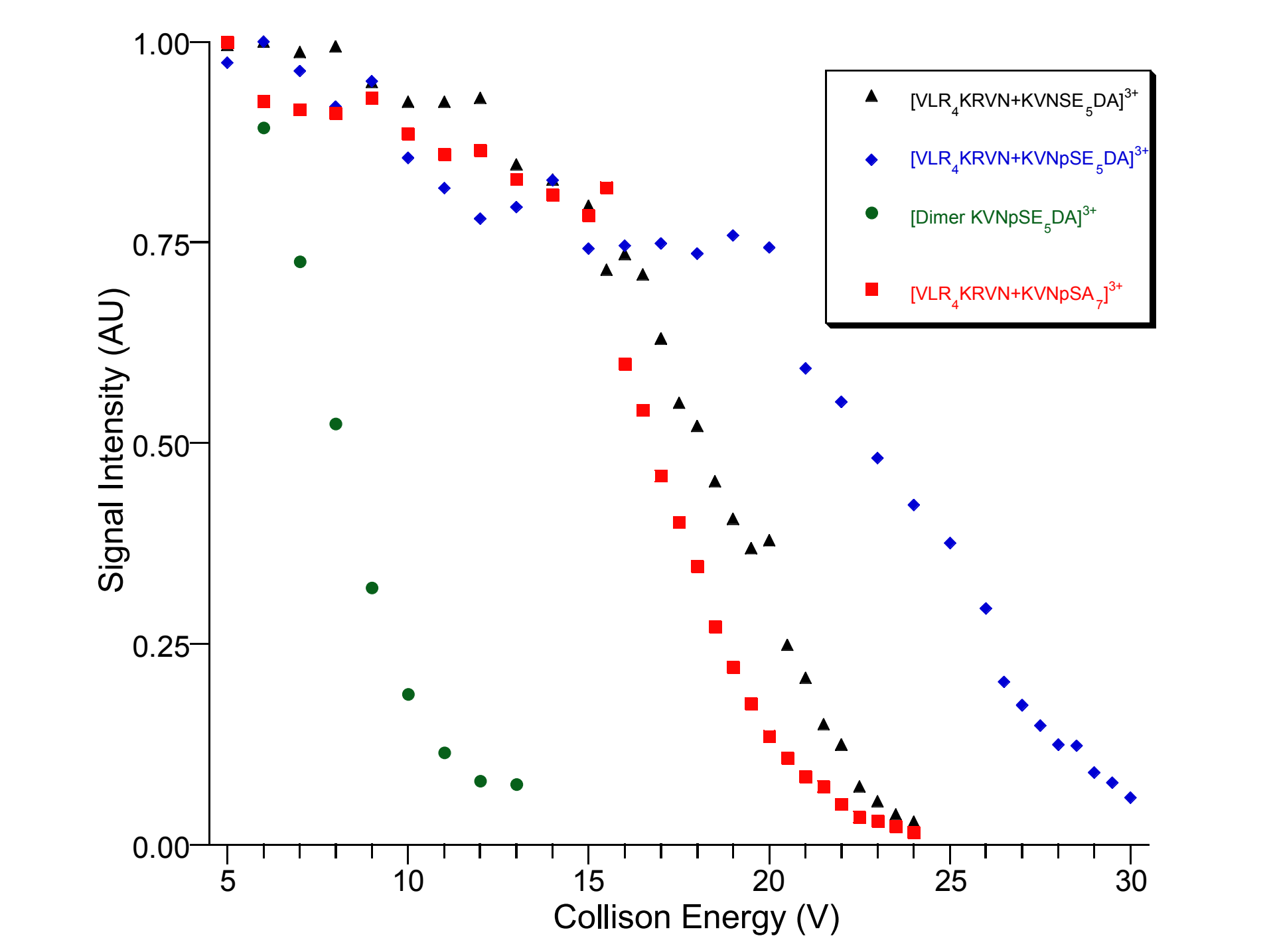
1.00
0.75
0.50
0.25
0.00
Signal Intensity (AU)
5
10
15
20
25
30
Collison Energy (V)
[VLR4KRVN+KVNSE5DA]3+
[VLR4KRVN+KVNpSE5DA]3+
[Dimer KVNpSE5DA]3+
[VLR4KRVN+KVNpSA7]3+

Estimation of Differences in NCX Binding Energies

In order to estimate the the binding energy of the NCX ions, we assume that the collision energy required to completely dissociate an ion complex is a measure of the enthalpy change of the reaction:

AB^+ + m ----------> products + m

That is, we consider only the disappearance of the complex ion and do not follow the various reaction products at all.

Estimation of binding energies from the collision data was carried out in a manner analogous to a method used for the determination of ion appearance potentials, the critical slope method pioneered by Honig and described further by Field and Franklin. In this approach, the rapidly changing portion of the dissociation curve is plotted as the logarithm of normalized ion intensity vs collision energy and fit with a linear regression.

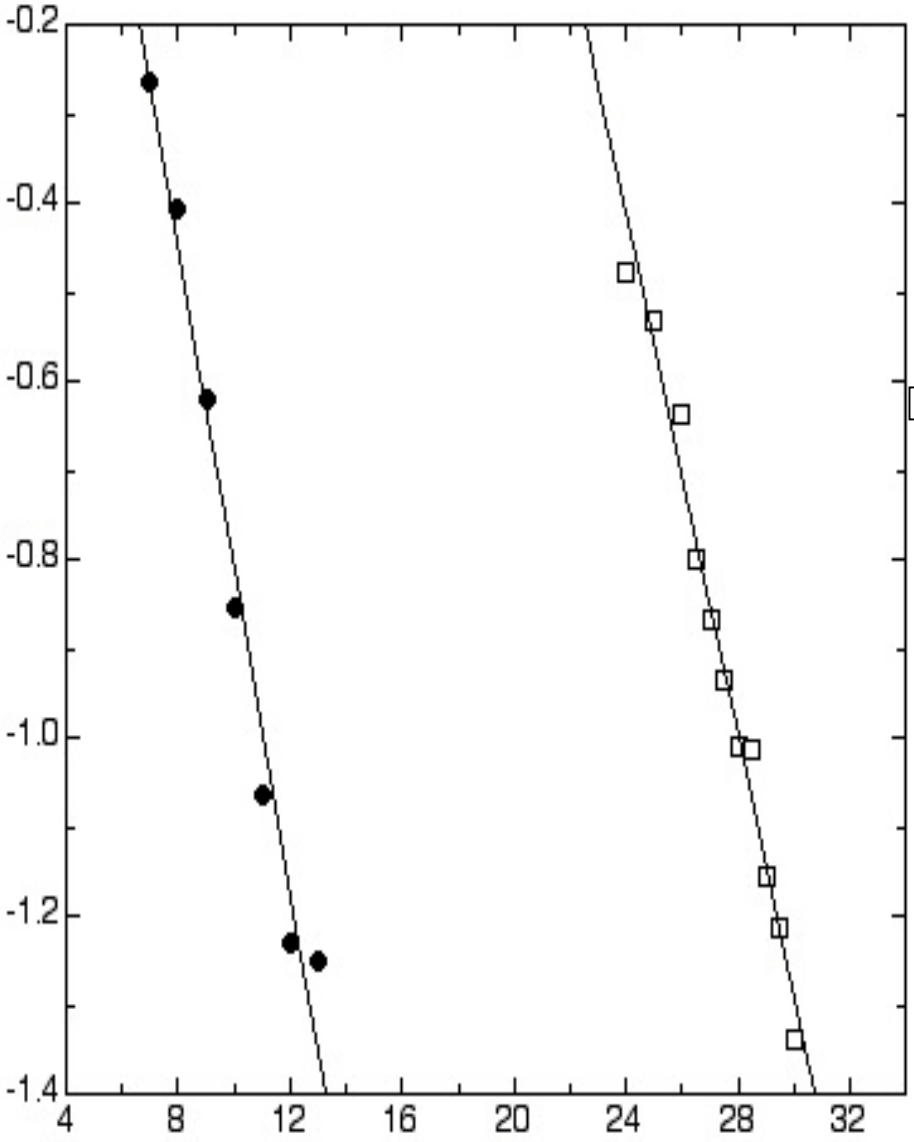

Collison Energy (eV-Lab),

• Dimer of KVNpSE5DA: Y = 0.990-0.180x

□ VLR4KRVN+KVNpSE5DA: Y = 3.089-0.146x

Plot of the log of normalized ion intensity for [Dimer of KVNpSE5DA]3+ and [VLR4KRVN+KVNpSE5DA]3+ versus collision energy fit with linear regression.

Table 2. Regression Parameters and Energy Differences for Dissociation Curves.

	a_0	a_1	x_0 (eV)	Δx_0 (eV)	Δx_0 (kcal/mol)
Dimer of $KVNpSE_5DA$	0.990	0.180	12.145	-	-
$VLR_4KRVN+KVNpSE_5DA$	3.089	0.146	29.377	17.2	396.3
$VLR_4KRVN+KVNSE_5DA$	3.553	0.231	22.850	10.7	246.2
$VLR_4KRVN+KVNpSA_7$	4.076	0.221	21.507	9.4	215.3
$VLR_4KRVN+KVNpSE_5DA$ (adj)	0.122	0.095	11.321	-0.8	-18.9
Average a_1*		-0.195			
Rel Std Dev		0.20			

The most striking thing about Table 2 is the energy required to disrupt the non-covalent complexes. For comparison, the C-C triple bond in acetylene is 234 kcal/mole and the ionization potential of Ar is 15.8 eV. Clearly the energies involved with the dissociation of these gas phase complexes is extraordinarily high.

These energies are not simply a consequence of studying multiply charged complexes is eliminated by considering that the energies shown in the last two columns are differences relative to the triply charged homodimeric ion.

The addition of a phosphate group increases the strength of the interaction by ~ 60%

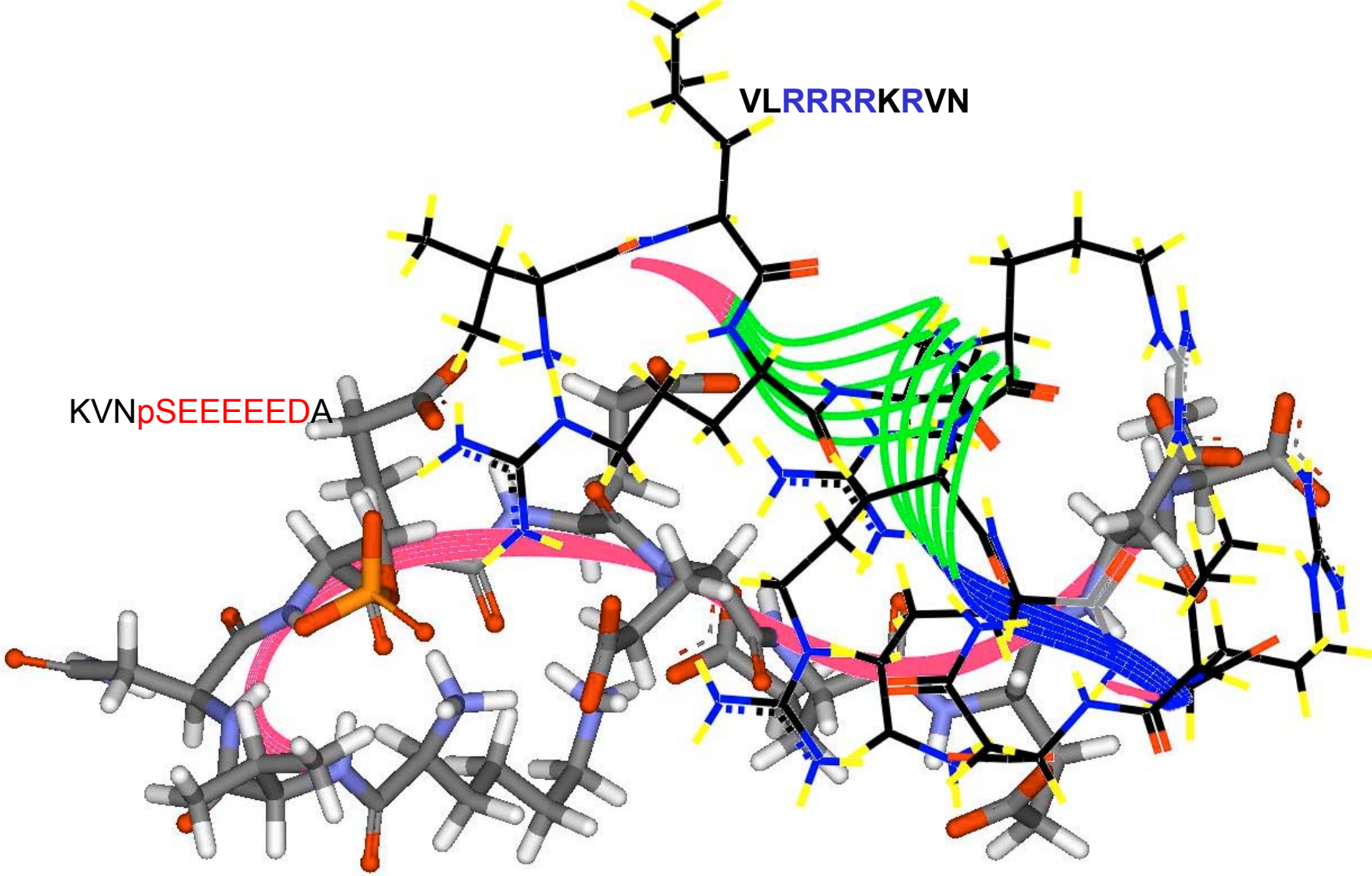

Molecular model of the NCX between KVNpSEEEEEDA (tubes) and VLRRRRKRVN (line). The structural motifs of the peptides are color-coded on ribbons superimposed along their backbones: pink for coil, green for helix, and blue for turn. Modeled by Accelrys DS Modeling 1.1 Suite running CHARMm force field.

ChelpG Atomic Charge Calculation

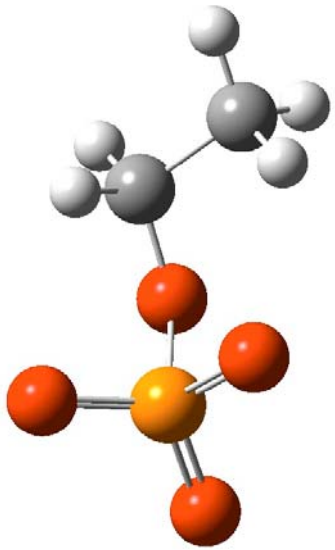

Calculations by Gaussian 03W using
DFT/B3LYP 6-31+ G(d,P)

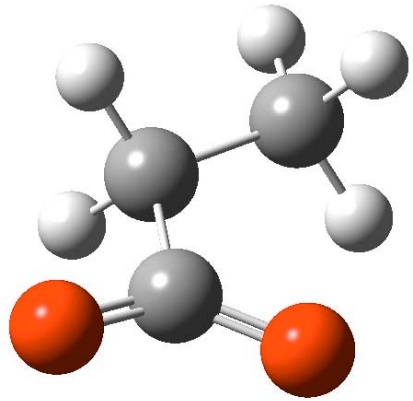

$CH_3CH_2OPO_3^{-2}$

APT Atomic Charges on O atoms in PO_3^{-2}: -1.1254 and –1.1457

$CH_3CH_2COO^-$

APT Atomic Charges on O atoms in COO^-: -0.998 and –1.042

- Electrostatically, O atoms on the phosphate group carry more negative charge than those on the carboxyl group.
- Geometrically, phosphate group could further away from side chain.
- Conformational change of acidic epitope by the negative charges on the phosphate group, which repulse the carboxyl groups further away from each other and relax the helical structure for interaction with the guanidinium groups on the basic epitope.

Results

- Significant increase in stability of NCX between epitopes by presence of phosphorylated residue.

- Stability of NCXs (from most stable to least stable) of VLRRRRKRVN with the acidic epitopes
  - KVNpSEEEEEDA> KVNSEEEEEDA> KVNpSAAAAAAA
  - one PO_3 residue+six acidic aa > six acidic aa > one PO_3 residue

Fragmentation Patterns of the Phosphate-Arginine Non-covalent Bond

- Investigate the gas-phase dissociation pathways of the phosphate-arginine electrostatic interaction.

- VLRRRRKRVN: basic epitope from the third intracellular loop of the dopamine D_2 receptor.

- SVSTDpTpSAE: epitope from the cannabinoid CB1 carboxyl terminus.

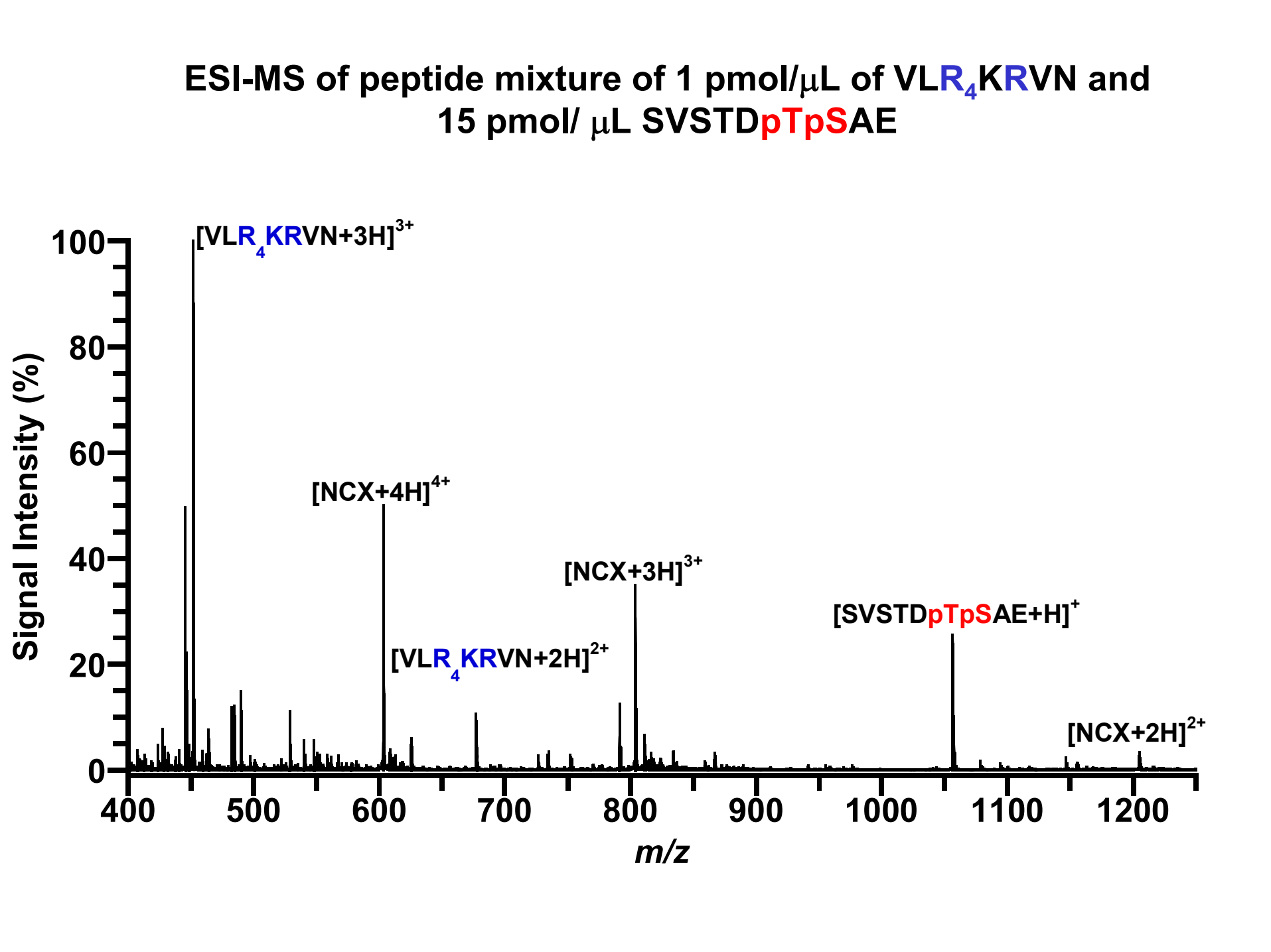
ESI-MS of peptide mixture of 1 pmol/μL of VLR4KRVN and
15 pmol/ μL SVSTDpTpSAE
[VLR4KRVN+3H]3+
[NCX+4H]4+
[NCX+3H]3+
[SVSTDpTpSAE+H]+
[VLR4KRVN+2H]2+
[NCX+2H]2+
Signal Intensity (%)
m/z
0
20
40
60
80
100
400
500
600
700
800
900
1000
1100
1200

ESI-MS/MS spectra of $[NCX+3H]^{3+}$ mass peak at a collision energy of 30 V.

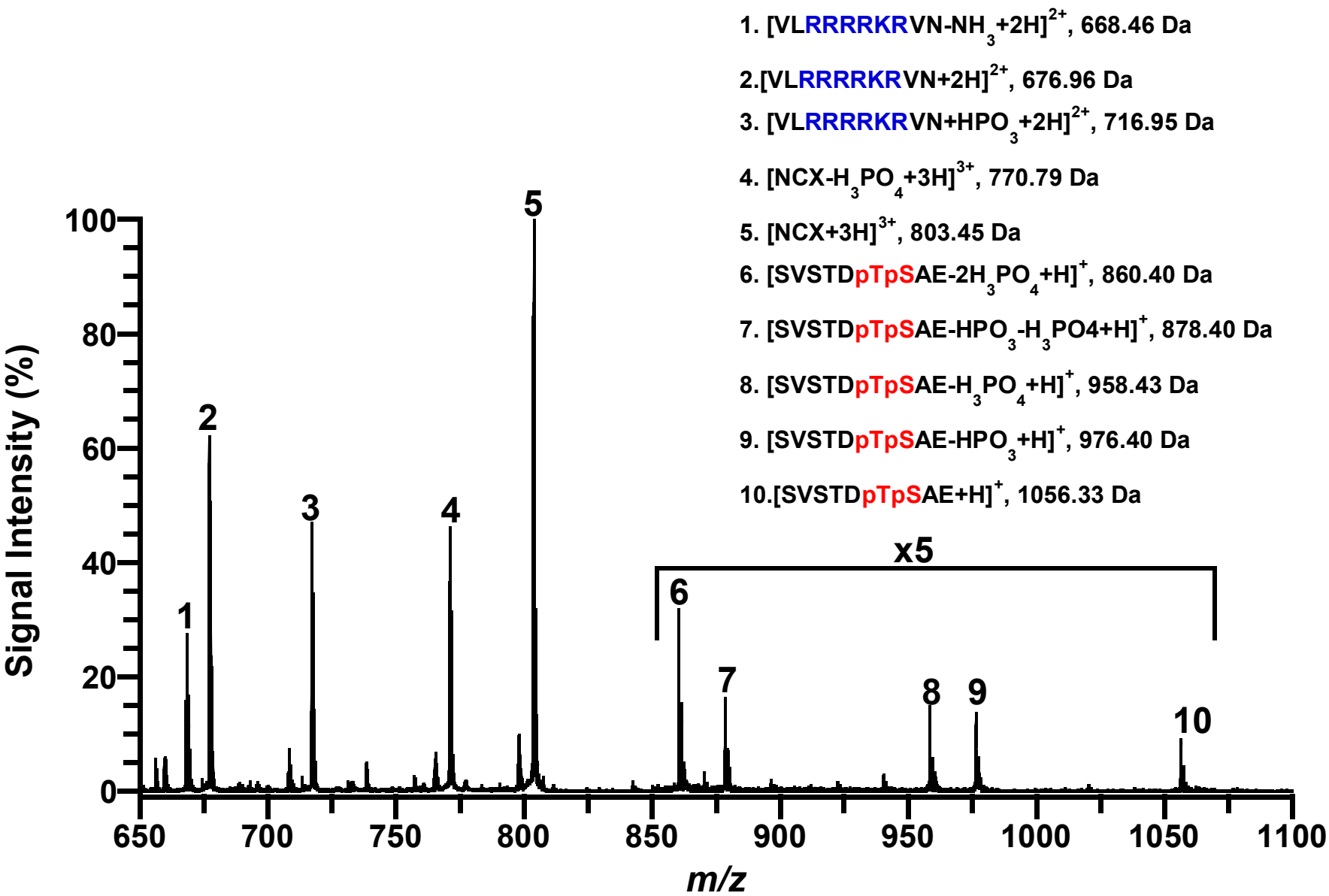

Ion Chromatograph of $[NCX+3H]^{3+}$

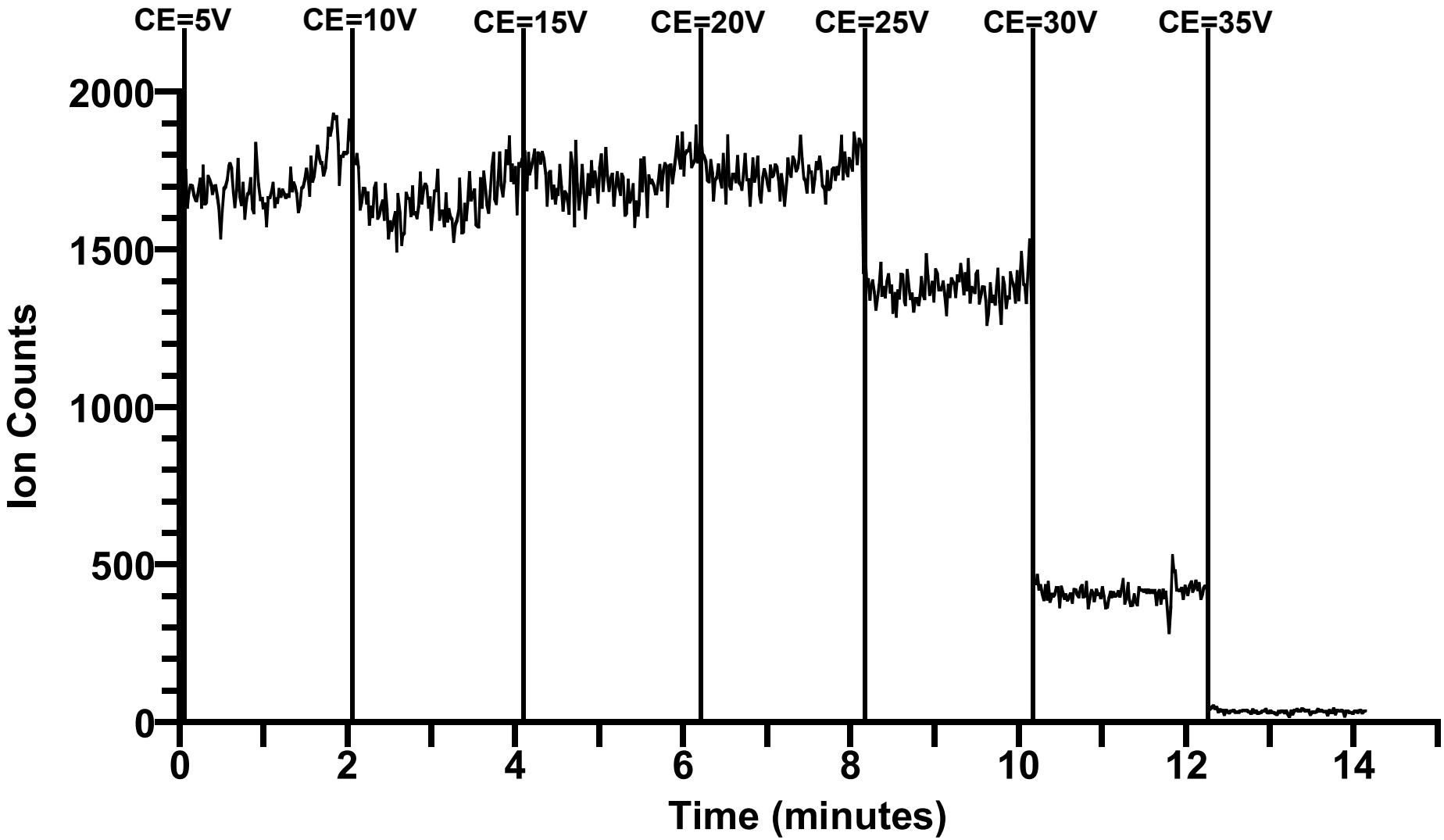

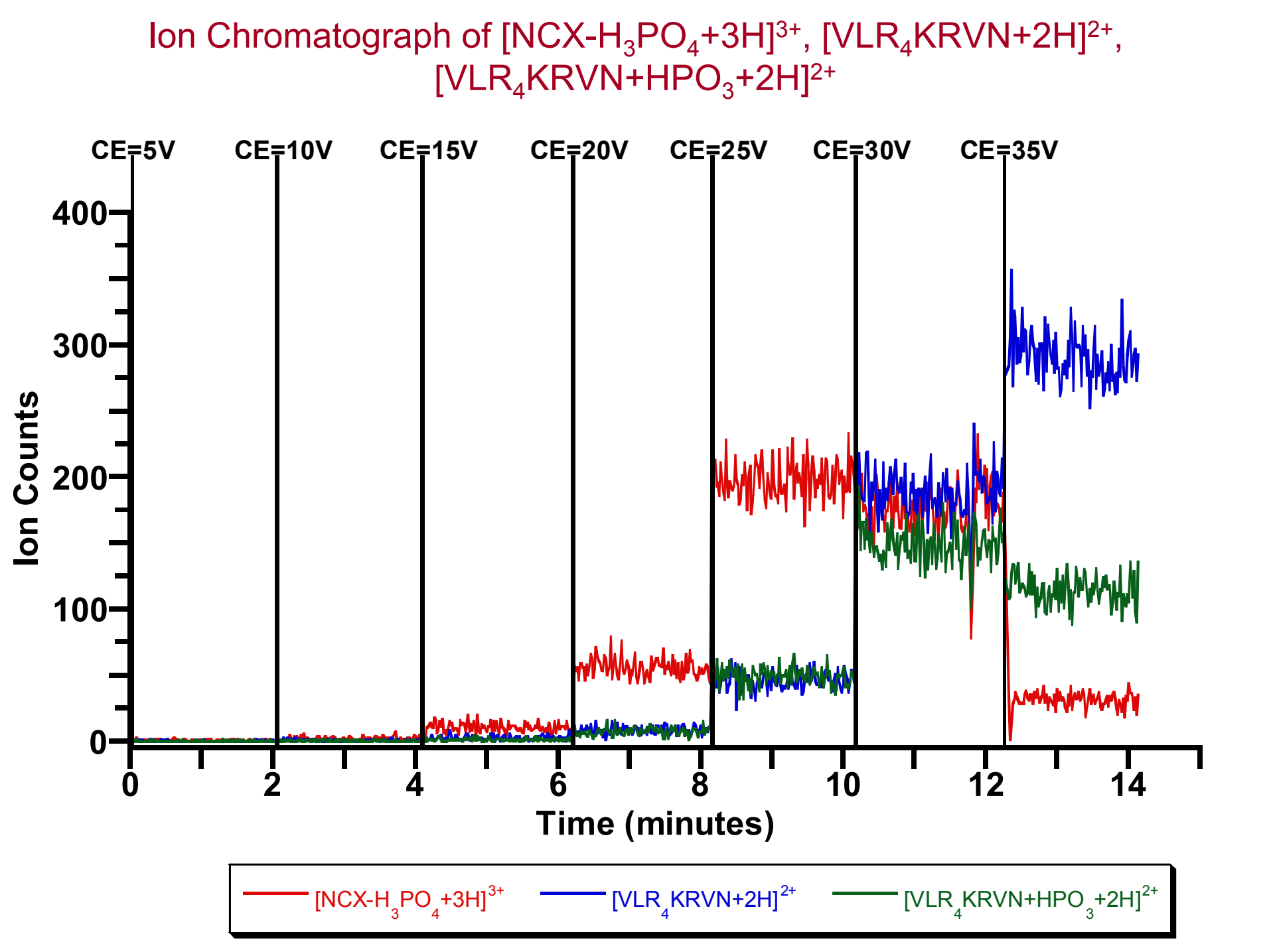
Ion Chromatograph of [NCX-H3PO4+3H]3+, [VLR4KRVN+2H]2+, [VLR4KRVN+HPO3+2H]2+
CE=5V
CE=10V
CE=15V
CE=20V
CE=25V
CE=30V
CE=35V
Ion Counts
0
100
200
300
400
0
2
4
6
8
10
12
14
Time (minutes)
[NCX-H3PO4+3H]3+
[VLR4KRVN+2H]2+
[VLR4KRVN+HPO3+2H]2+

MS Spectrum

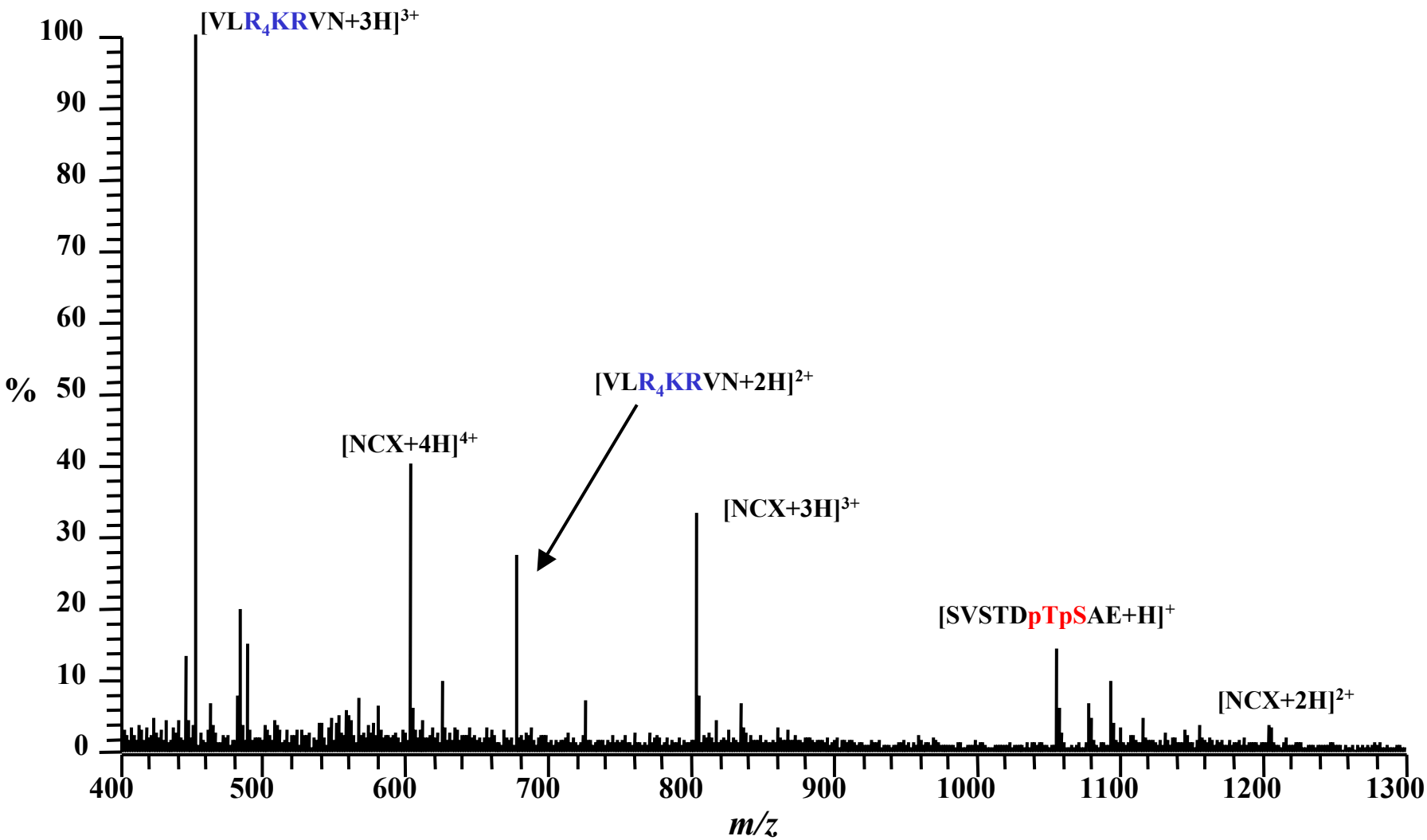

ESI-ion trap mass spectrum of a peptide mixture consisting of 1 pmol/μL of VLRRRRKRVN and 15 pmol/μL of SVSTDpTpSAE.

MS^2 Spectrum of $[NCX+3H]^{3+}$

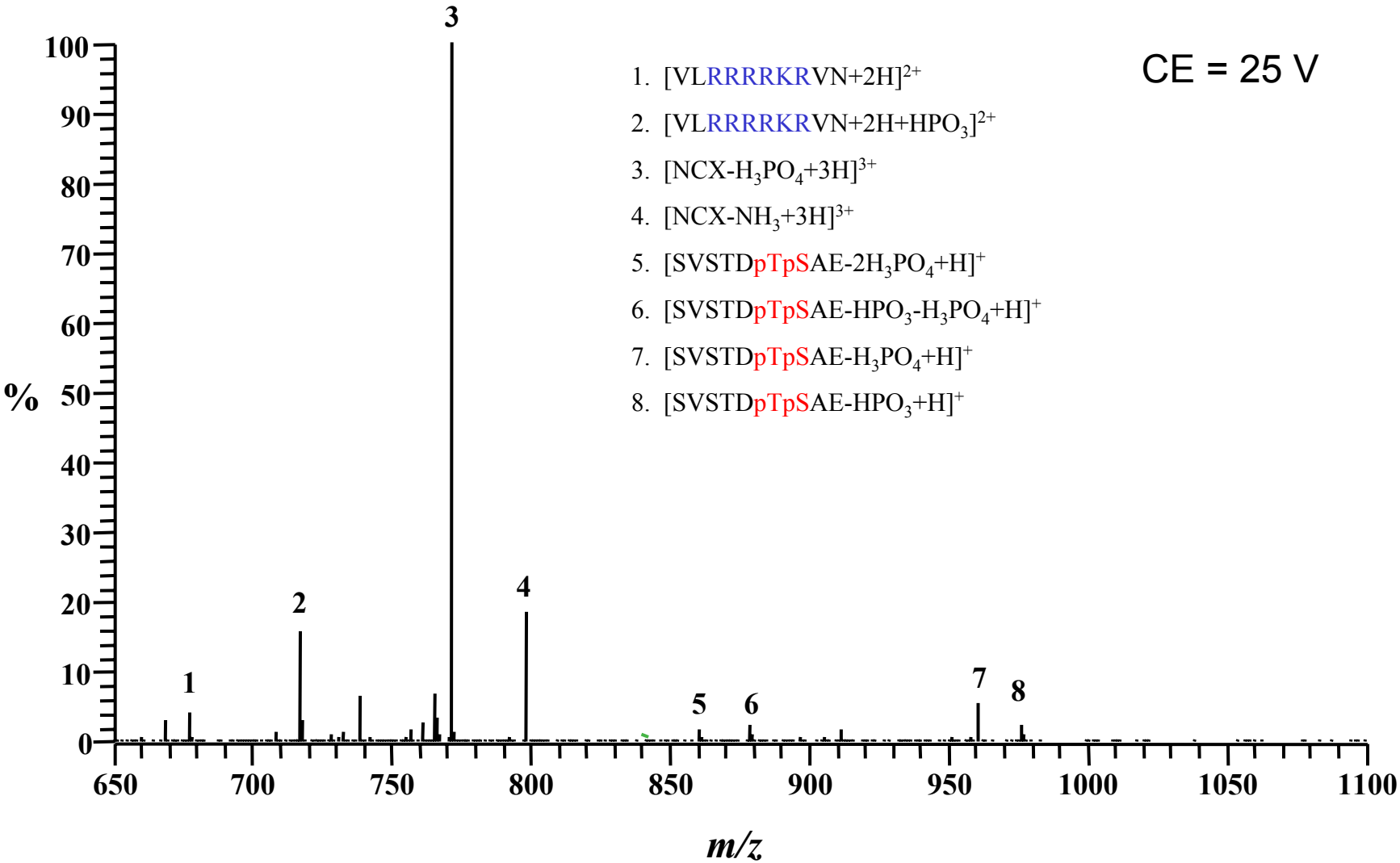

ESI-ion trap mass spectrum of a peptide mixture consisting of 1 pmol/μL of VLRRRRKRVN and 15 pmol/μL of SVSTDpTpSAE.

MS^3 Spectrum of $[VLR_4KRVN+2H]^{2+}$

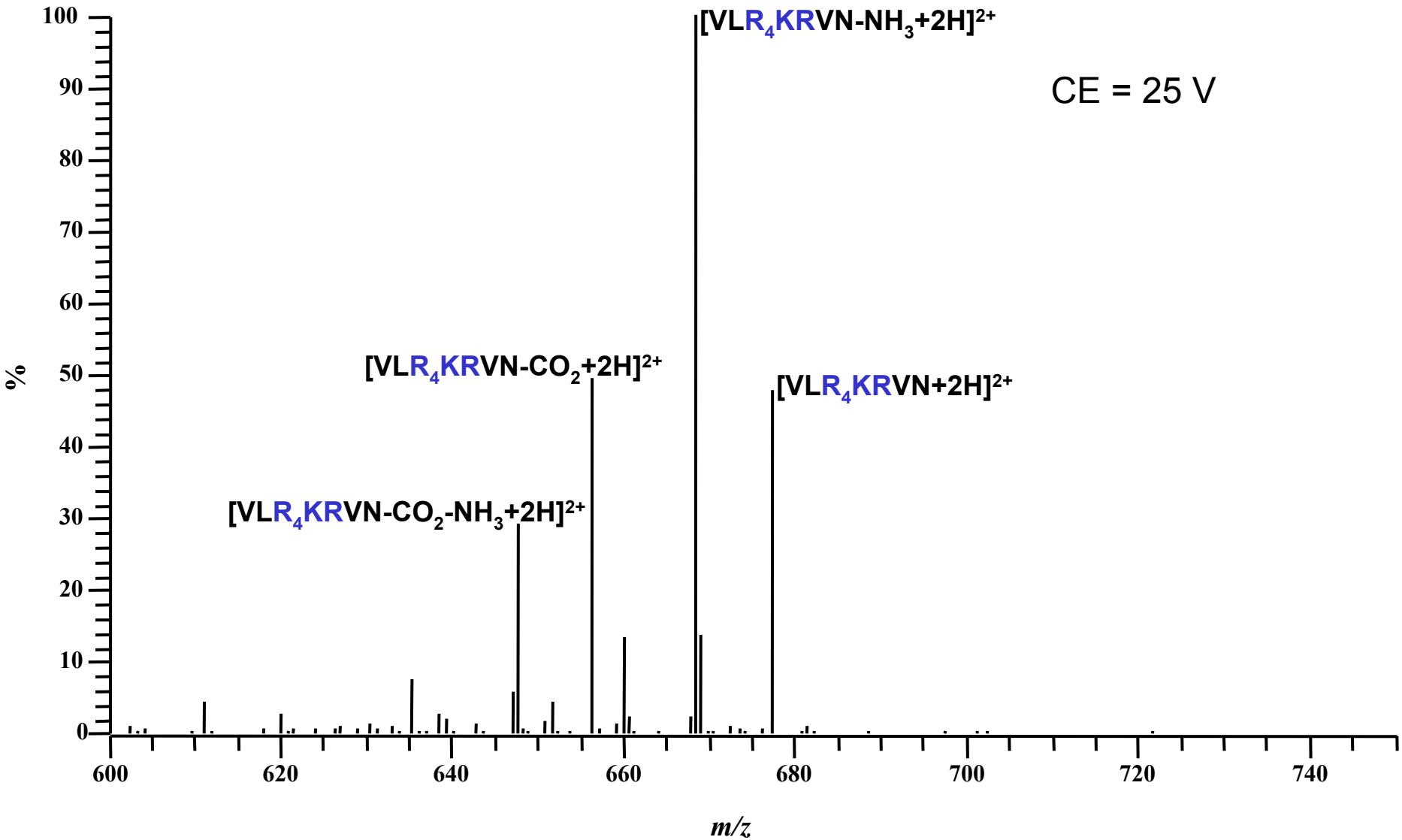

ESI-ion trap mass spectrum of a peptide mixture consisting of 1 pmol/μL of VLRRRRKRVN and 15 pmol/μL of SVSTDpTpSAE.

MS^3 Spectrum of $[VLR_4KRVN+HPO_3+2H]^{2+}$

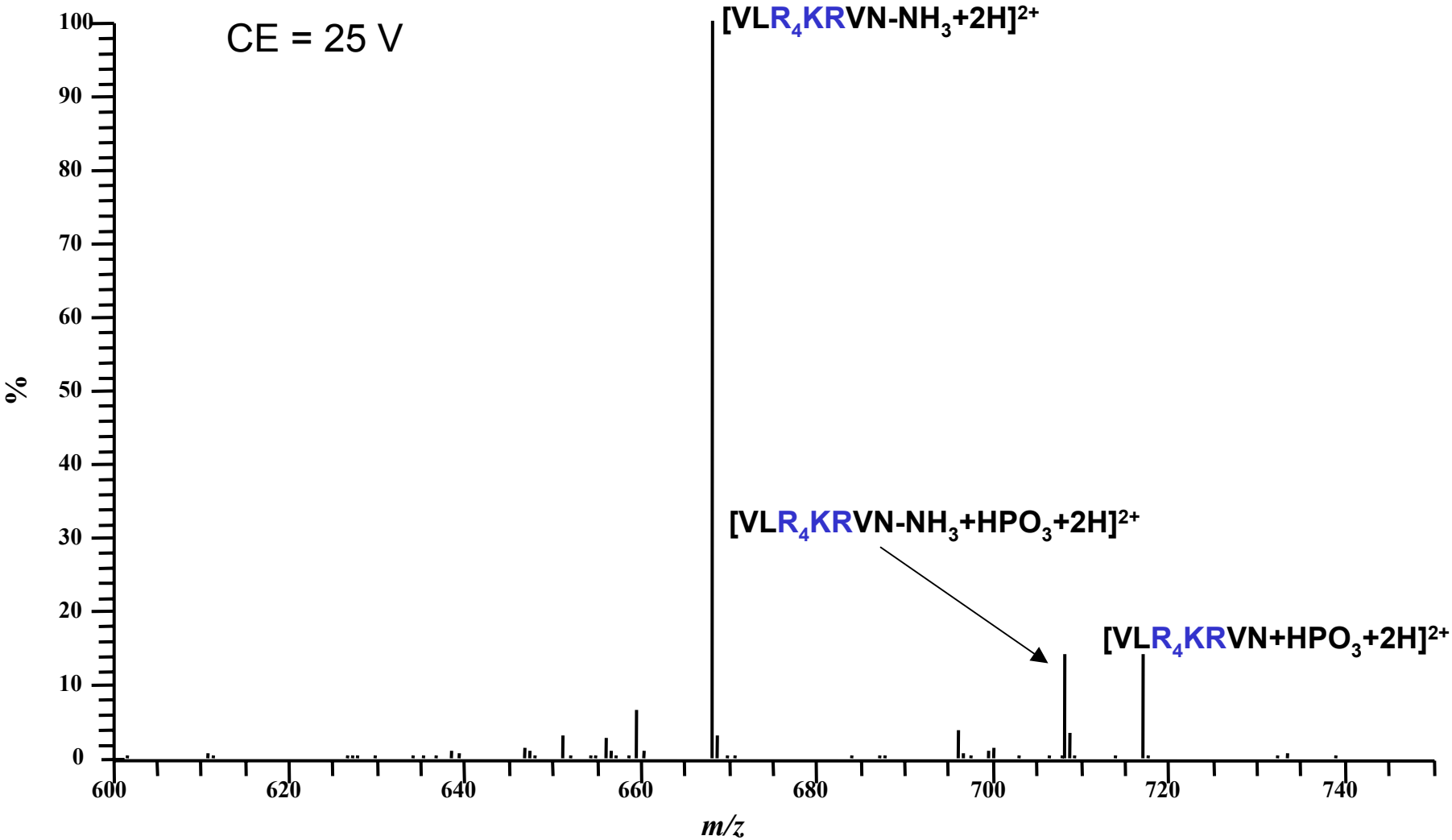

ESI-ion trap mass spectrum of a peptide mixture consisting of 1 pmol/μL of VLRRRRKRVN and 15 pmol/μL of SVSTDpTpSAE.

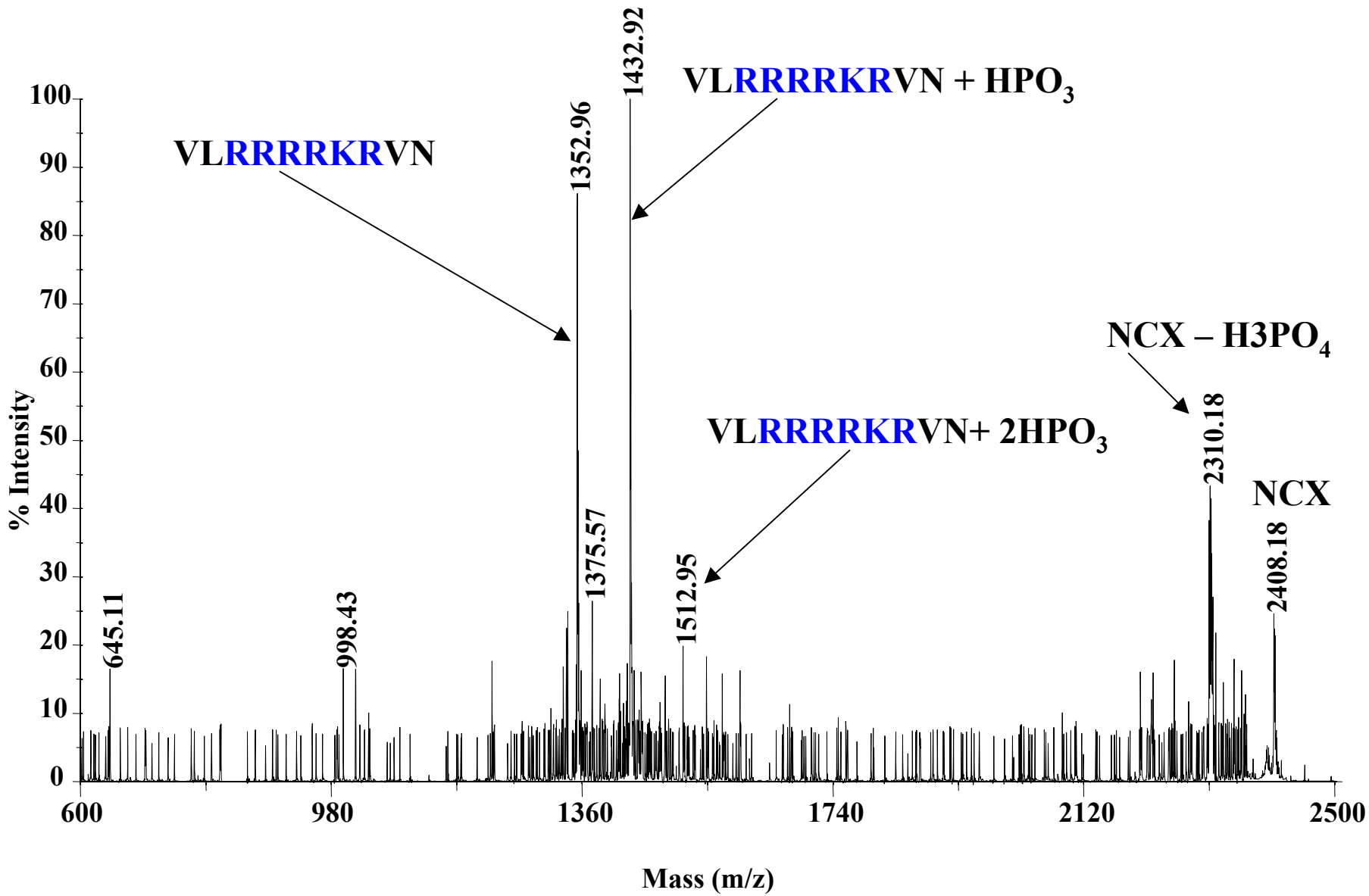
CID of the NCX of VLRRRRKRVN + SVSTDpTpSAE (MALDI TOF-TOF)
VLRRRRKRVN
VLRRRRKRVN + HPO3
NCX – H3PO4
VLRRRRKRVN+ 2HPO3
NCX
1432.92
1352.96
2310.18
1375.57
1512.95
2408.18
645.11
998.43
% Intensity
Mass (m/z)
100
90
80
70
60
50
40
30
20
10
0
600
980
1360
1740
2120
2500

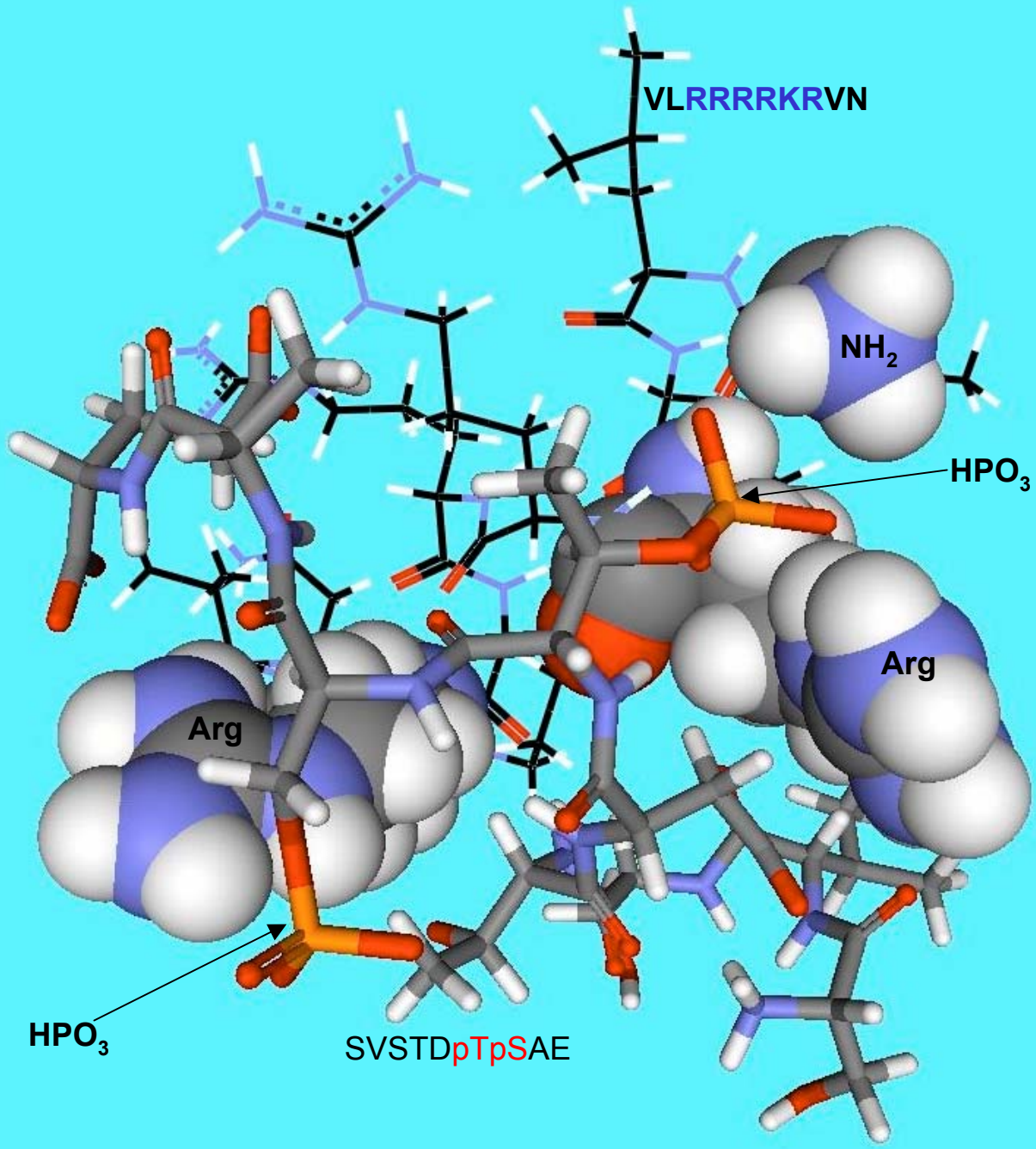
VLRRRRKRVN
NH2
HPO3
Arg
Arg
HPO3
SVSTDpTpSAE

Results

Two Dissociation Pathways for NCX

- Major pathway: Disruption of the electrostatic interactions between Arg residues and the phosphate groups. Results in intact VLRRRRKRVN and SVSTDpTpSAE mass peaks.

- Alternative pathway: NCX is dissociated along the covalent bond between the oxygen from either Thr or Ser and HPO_3. Pathway demonstrates the stability of the electrostatic interaction between phosphorylated residues and Arg residues in the gas-phase.

Human Dopamine D2 Receptor (443 aa, MW: 50619 Da) inhibits the release of dopamine.

```
MDPLNLSWYD DDLERQNWSR PFNGSDGKAD RPHYNYYATL LTLLIAVIVF GNVLVCMAVS      60
REKALQTTTN YLIVSLAVAD LLVATLVMPW VVYLEVVGEW KFSRIHCDIF VTLDVMMCTA     120
SILNLCAISI DRYTAVAMPM LYNTRYSSKR RVTVMISIVW VLSFTISCPL LFGLNNADQN     180
ECIIANPAFV VYSSIVSFYV PFIVTLLVYI KIYIVLRRRRKRVNTKRSSR AFRAHLRAPL     240
KGNCTHPEDM KLCTVIMKSN GSFPVNRRRV EAARRAQELE MEMLSSTSPP ERTRYSPIPP     300
SHHQLTLPDP SHHGLHSTPD SPAKPEKNGH AKDHPKIAKI FEIQTMPNGK TRTSLKTMSR     360
RKLSQQKEKK ATQMLAIVLG VFIICWLPFF ITHILNIHCD CNIPPVLYSA FTWLGYVNSA     420
VNPIIYTTFN IEFRKAFLKI LHC                                             443
```

Human Adenosine A2A Receptor (412 aa, MW 44707 Da) is a member of the G-protein coupled receptor family. Its activation stimulates cyclic AMP production.

```
MPIMGSSVYI TVELAIAVLA ILGNVLVCWA VWLNSNLQNV TNYFVVSLAA ADIAVGVLAI      60
PFAITISTGF CAACHGCLFI ACFVLVLTQS SIFSLLAIAI DRYIAIRIPL RYNGLVTGTR     120 AKGIIAICWV
LSFAIGLTPM LGWNNCGQPK EGKNHSQGCG EGQVACLFED VVPMNYMVYF        180 NFFACVLVPL
LLMLGVYLRI FLAARRQLKQ MESQPLPGER ARSTLQKEVH AAKSLAIIVG        240 LFALCWLPLH
IINCFTFFCP DCSHAPLWLM YLAIVLSHTN SVVNPFIYAY RIREFRQTFR        300 KIIRSHVLRQ
QEPFKAAGTS ARVLAAHGSD GEQVSLRLNG HPPGVWANGS APHPERRPNG     360 YALGLVSGGS
AQEpSQGNTGL PDVELLSHEL KGVCPEPPGL DDPLAQDGAG VS   412
```

heteromerization depends on an electrostatic interaction between an Arg-rich epitope from the third intracellular loop of the D_2 receptor

And $DD_{401\text{-}402}$ or a phosphorylated Ser pS_{374} in the C-terminus of the A_2A receptor.

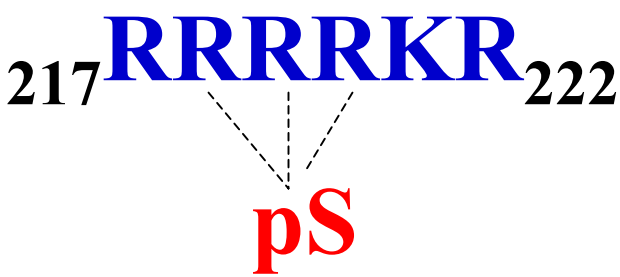

D2R epitopes

From	Sequence	res #
Human	VL**RRRRKR**VN	215-224
Green Monkey	VL**RRRRKR**VN	215-224
Bovine	VL**RRRRKR**VN	215-224
Mouse	VL**RKRRKRV**N	215-224
Rat	VL**RRRRKR**VN	215-224
Turkey	VL**RKRRKR**VN	215-224
Frog	VL**RKRRKR**VN	208-218

Table 1. Interspecies comparison of the A2AR

A2AR first carboxyl terminal epitope

From	Sequence	res #
Human	**SAQEpSQGNT**	370-378
Guinea Pig	**SAQRpSGDAS**	367-376
Rat	**SAQGpSPRDV**	365-373
Mouse	**STQGpSPGDV**	365-373
Dog	**IAPEpSHGDM**	370-378

A2AR second carboxyl terminal epitope

From	Sequence	res #
Human	**HEL KGVCPEPPGLDDPLAQDGAGVS**	388-412
pig	**HEHKGTCPESPSLEDPPAHGGAGVS**	385-409
Mouse	**HPGLG DHLAQGRVGTASWSSEFAPS**	386-410
Rat	**HPGLR GHLVQARVGASSWSSEFAPS**	386-410
Dog	**HEL KGACPESPGLEGPLAQDGAGVS**	388-412

Schematic of the GST-A2A$_{CT}$ fusion protein. The underlined sequence corresponds to the two A2AR epitopes.

D2 epitope

Woods et al *Anal Chem* (2004)

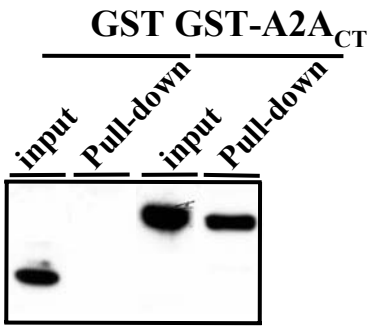

Association of the GST-A2ACT to the D2R epitope. Increasing concentrations of the GST-A2ACT were incubated with Sepharose-D2R epitope. After the pull-down experiment, protein bound to D2R epitope was resolved by SDS-PAGE and immunoblotted

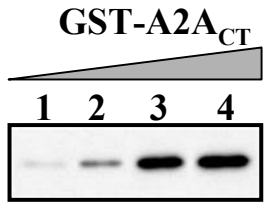

GST and GST-A2ACT pull-down experiment. 50 ng of GST or GST-A2ACT proteins (see input) were incubated with the D2R epitope coupled to Sepharose-4B. After the pull-down experiment proteins bound to the D2R-epitope were resolved by SDS-PAGE and immunoblotted using a polyclonal anti-GST antibody (1/200).

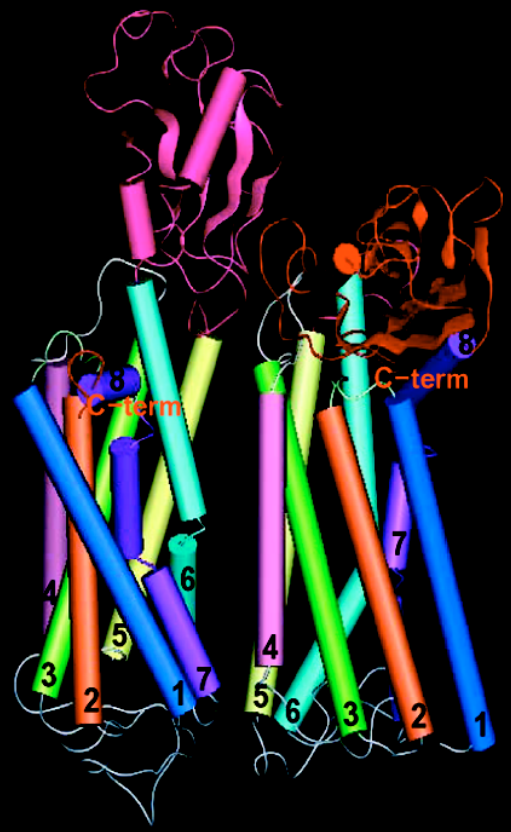

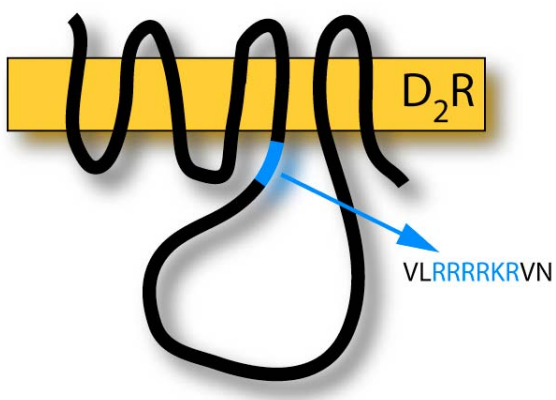

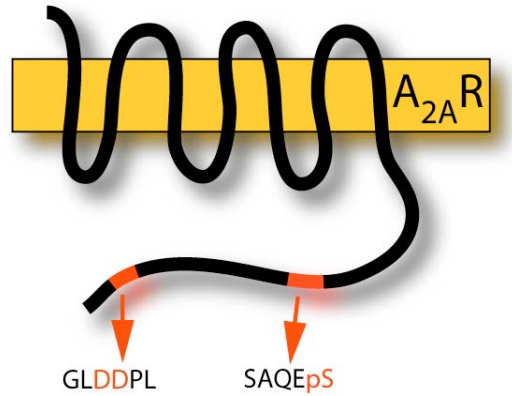

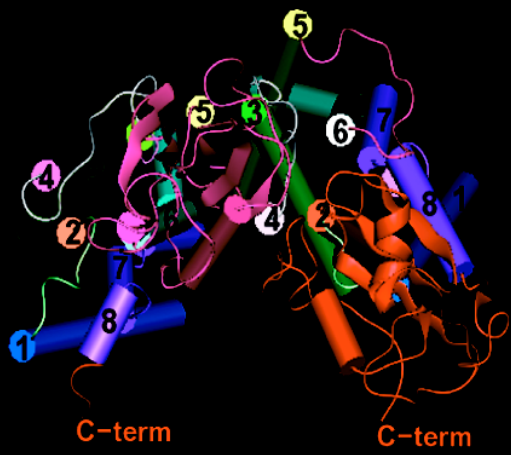

Canals et al., Nov. (2003)
J. Biol. Chem.

Table I. Formation of peptide-peptide complexes

Mixture	Complex
SAQEpSQGNT + VLRRRRKRVN	Yes
SAQEpSQGNT + VLAAAAKAVN	No
SAQESQGNT + VLRRRRKRVN	No
SAQESQGNT + VLAAAAKAVN	No
HELKGVCPEPPGLDDPLAQDGAGVS + VLRRRRKRVN	Yes
HELKGVCPEPPGLDDPLAQDGAGVS + VLAAAAKAVN	No
HELKGVCPEPPGLAAPLAQDGAGVS + VLRRRRKRVN	No
HELKGVCPEPPGLAAPLAQDGAGVS + VLAAAAKAVN	No
EKEVESENEAD + VLRRRRKRVN	No
EKEVESENEAD + VLAAAAKAVN	No

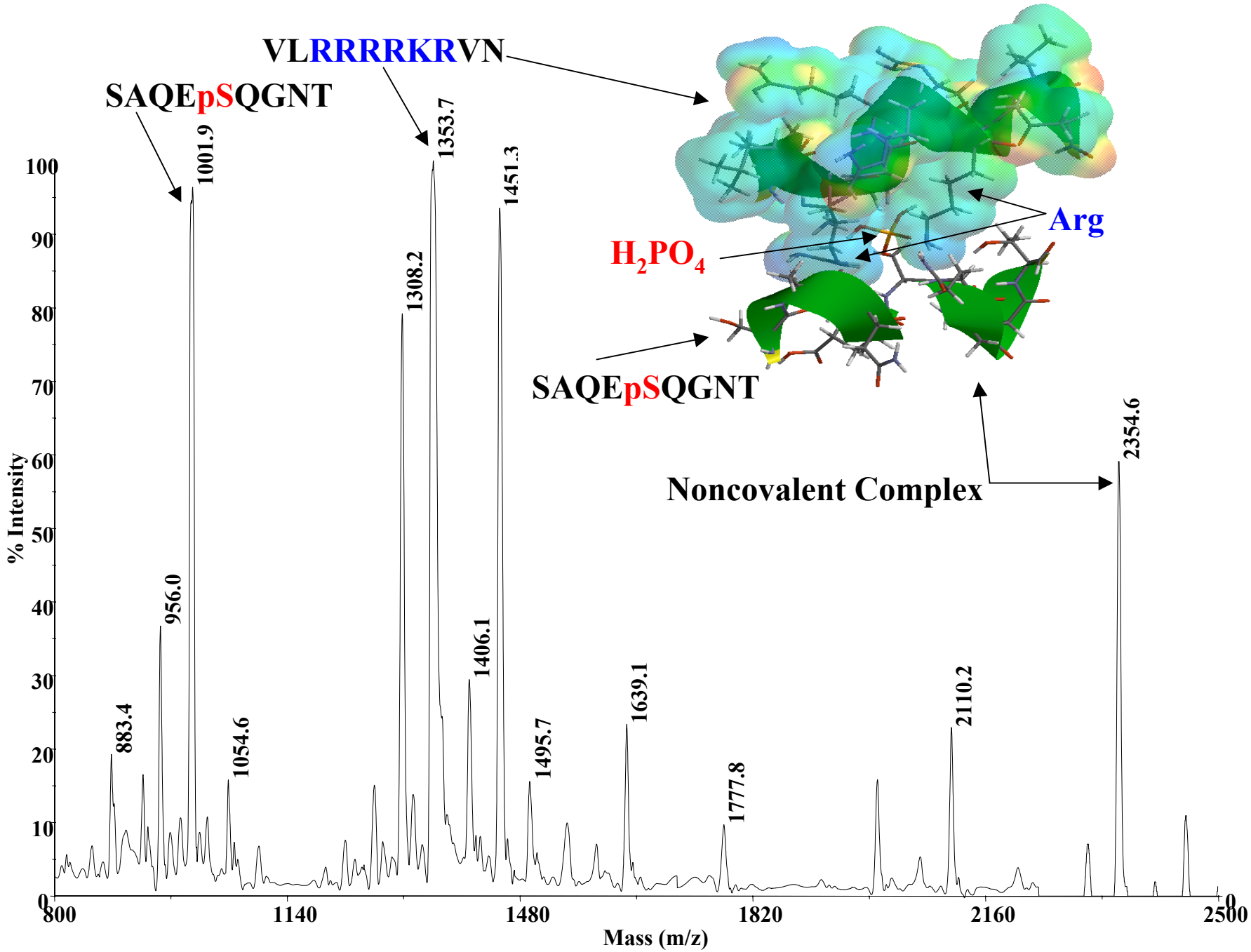
VLRRRRKRVN
SAQEpSQGNT
1001.9
1353.7
1451.3
1308.2
956.0
1406.1
883.4
1054.6
1495.7
1639.1
1777.8
2110.2
2354.6
Arg
H_2PO_4
SAQEpSQGNT
Noncovalent Complex
% Intensity
Mass (m/z)
100
90
80
70
60
50
40
30
20
10
0
800
1140
1480
1820
2160
2500

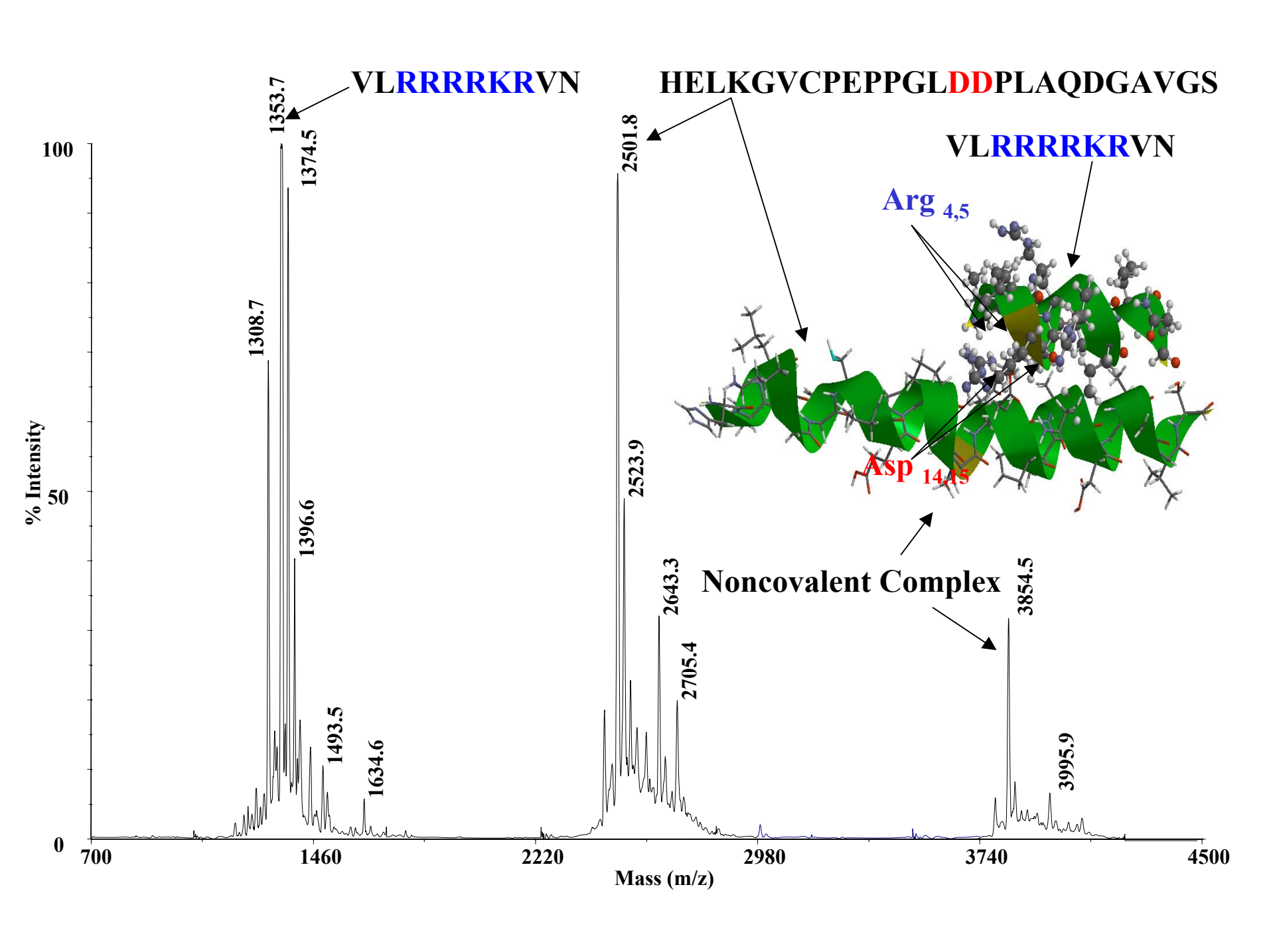
VLRRRRKRVN
HELKGVCPEPPGLDDPLAQDGAVGS
VLRRRRKRVN
Arg 4,5
Asp 14,15
Noncovalent Complex
1353.7
1374.5
2501.8
1308.7
2523.9
1396.6
2643.3
2705.4
1493.5
1634.6
3854.5
3995.9
100
50
0
% Intensity
700
1460
2220
2980
3740
4500
Mass (m/z)

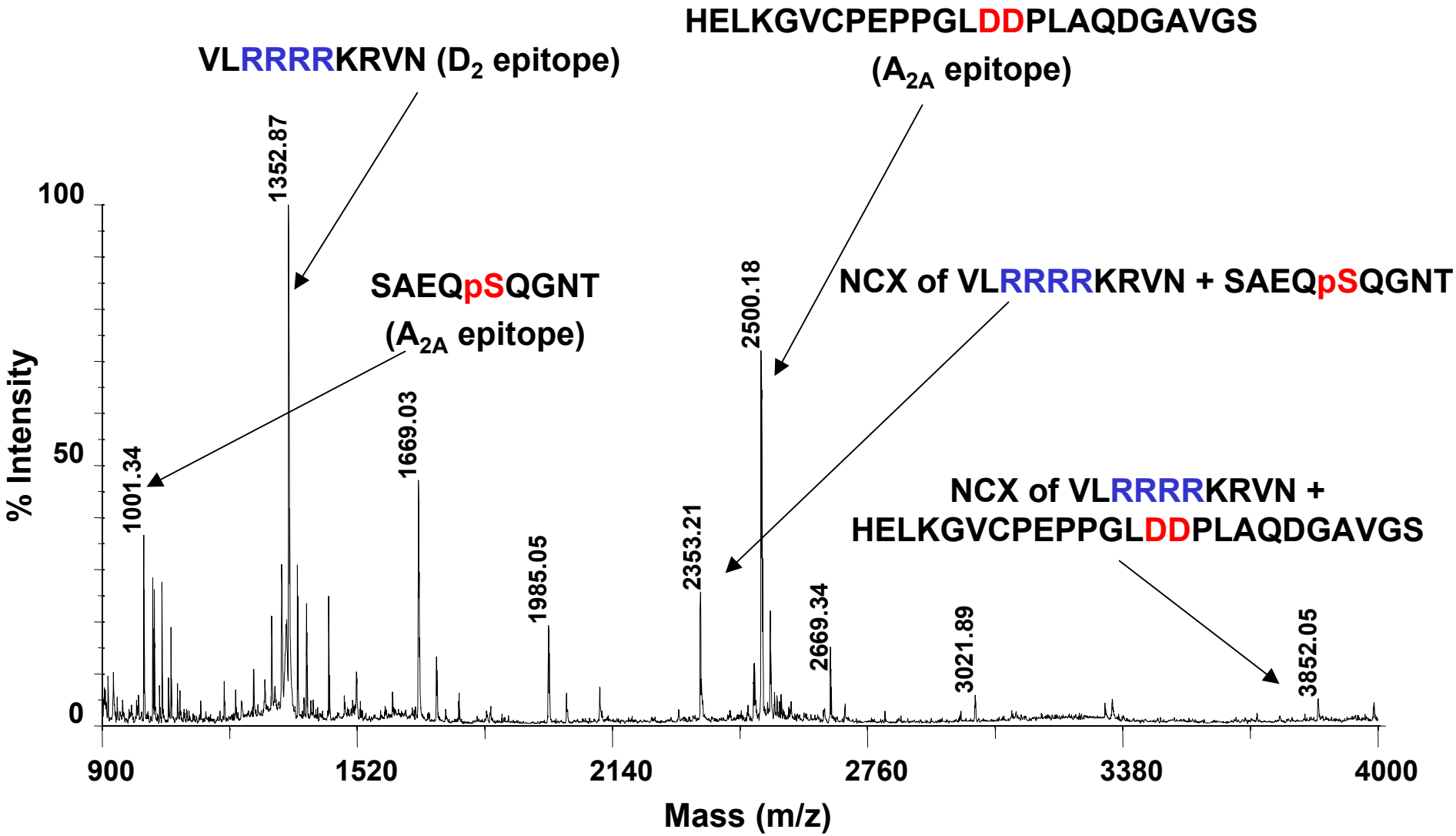

Normalized relative abundance of the MH^+ of NCX between D_2 epitope with the phosphorylated (70%) and the nonphosphorylated (5%) A_{2A} epitope.

Acknowledgements

Amina S Woods

Hay-Yan J Wang

Alfred Yergey

Sergi Ferre

Robert Cole

Robert O’Meally

NIDA-IRP, NIH

ONDCP